〔논문〕 한국수소에너지학회지
J. of the Korean Hydrogen Energy Society
Vol. 6. No. 1(1995)

Ni분말과 소결시킨 $V_{0.9}Ti_{0.1}$ 수소저장합금의 전극특성

김동명, 이한호, 이기영, 이재영

The Electrode Characteristics and Modified Surface Properties of $V_{0.9}Ti_{0.1}$ Alloy Sintered with Ni Powder

Dong-Myung Kim, Han-Ho Lee, Ki-Young Lee and Jai-young Lee

Dept. of Materials Science and Engineering,
Korea Advanced Institute of Science & Technology,
Kusung-dong 373-1, Yusung-gu, Taejon, Korea

초 록 : $V_{0.9}Ti_{0.1}$ 합금은 많은 양의 수소를 흡수할 수 있으나 KOH 전해질내에서 방전이 되지 않기 때문에 Ni-MH 전지의 음극재료로 사용할 수 없었다. 이와 같은 $V_{0.9}Ti_{0.1}$ 합금을 전해질내에서 수소 흡수/방출에 대한 촉매효과를 갖도록 Ni 분말과 소결하였다.

Ni 분말과 소결한 모든 시편은 KOH 전해질내에서 10 Cycle 이내에 활성화 되었다. 방전용량은 소결시 첨가된 Ni 분말의 양에 따라 maximum 거동을 보였다. 가장 높은 방전용량을 보여준 전극의 경우는 소결시 첨가된 Ni 분말의 양이 25wt.%이며 그 방전용량은 302mAh/g이었다. SEM과 EDS 그리고 XRD 분석결과 소결시 VNi_3가 형성됨을 알 수 있었다. $V_{0.9}Ti_{0.1}$ 합금의 표면에 형성된 VNi_3는 전극의 최적방전조건과 밀접한 관련이 있음을 알 수 있었다. Brewer-Engel 이론에 의하면 VNi_3는 수소의 evolution에 대한 전기적 촉매효과가 매우 높다고 보고하고 있으며, 이러한 효과는 본 실험결과 교환전류밀도의 증가와 방전시 과전압의 감소로써 나타났다.

본 연구에서는 수소의 저장용량은 크나 KOH 전해질내에서 방전되지 않는 합금을 사용하여 Ni-MH 전지용 음극개발을 하기 위해 Ni분말과 소결하여 합금의 표면을 변화시키는 새로운 방법을 제안하고자 한다.

1. Introduction

The Nickel-Metal hydride(Ni-MH) batteries have received attention in recent years because of serveral advantages over nickel-cadmiun batteries; e. g., higher energy density, longer cycle life, the capability of overcharging and overdischarging, and absence of the poisinous heavy metal[1-3]. A lot of works[4-7] have been carried out to develop anode materials AB_2-type and AB_5-type MH alloys. In the alloy design, these MH alloys should contain nickel as a catalyst. The discharge capacity of AB_2-type and AB_5-type MH alloys are about 250mAh/g and 350 mAh/g, respectively due to the limited of nickel-containing alloy system.

It has not been tried so far to utilize the MH alloy which does not contain nickel. In this work, a new process has been introduced as a guideline to develop an anode material using a MH alloy which has large hydrogen storage capacity but cannot be discharged in KOH electrolyte.

$V_{0.9}Ti_{0.1}$ alloy is very attractive material for the anode of Ni-MH secondary battery because of its large hydrogen storage capacity[8]. However, the alloy has not been used for anode material because of its poor discharge behavior in KOH electrolyte. The $V_{0.9}Ti_{0.1}$ alloy powder and Ni powder have been sintered to modify the alloy surface by providing catalytic nickel layel on the surface. The dischange characteristics of $V_{0.9}Ti_{0.1}$ alloy has been investigated and the dischargeability has been drastically improved by the surface modification.

2. Experimental details

2-1 Preparation of the alloys and electrodes

$V_{0.9}Ti_{0.1}$ alloy were prepared by arc melting in an argon atomosphere. The alloys were turned over several times to get homogeneous structure. Then the alloy were mechanically purverized to prepare powder below 400mesh (less than 37 μm). The crystal structtures of the alloys were confirmed as BCC structure by X-ray analysis.

$V_{0.9}Ti_{0.1}$ alloy powders(37 μm) ans Ni powders (10 μm) were mixed together in the weight ratios of 1:1, 1:0.5, 1:0.125 and pressed to pellets with a diamater of 10mm and a thickness of about 1mm at the compacting pressure of 10tons/㎠, These pellets were sintered in a vacuum of about $10^{-2}\sim10^{-3}$ torr at 900℃ for 5min. In order to identify the crystal structures of the sintered electrodes, X-ray analysis was performed. The hydrogen storage performance was measured by determining P-C-T curves using Sievert's type apparatus. The surface morphology of the sintered electrodes was examined by SEM (Scanning Electron Microscopy) and their chemical composition was characterized by EDS analysis.

2-2 Electrochemical measurements

A half-cell was constructed using platinum wire as a counter electrode and mercury/mercury oxide (Hg/HgO) electrode as a

reference electrode in the 30wt% KOH electrolyte. The charge-discharge was controlled by the potential of the working electrode, i.e. sintered pellet, with respect to an reference electrode with an automatic galvanostatic charge-discharge apparatus. Cycle tests were conducted at 30℃ by repeatedlycharging and discharging at 50mA/g ($V_{0.9}Ti_{0.1}$ alloy) for 12h with a resting time of 30 seconds. The cutoff voltage was -0.75V v.s Hg/HgO. The discharge capacity was expressed in mAh(milliampere hours) per gram of $V_{0.9}Ti_{0.1}$ alloy.

It was shown that the kinetics of the charge -transfer reaction, i.e. exchange current density, was able to be characterized electrochemically using linear polarization method at OCP(Open-Circuit-Potential) between-10mV and+10mV.

3. Results and discussion

3-1. Activation of the sintered electrodes

The activation behavior of the electrodes is shown in Fig. 1. The electrode mixed with Ni powder and pressed without sintering was not activated even at 10th cycle. However, all of the electrodes sintered with Ni powder were fully activated within 10th cycle, Furthermore, the activation behavior was improved by increasing nickel content.

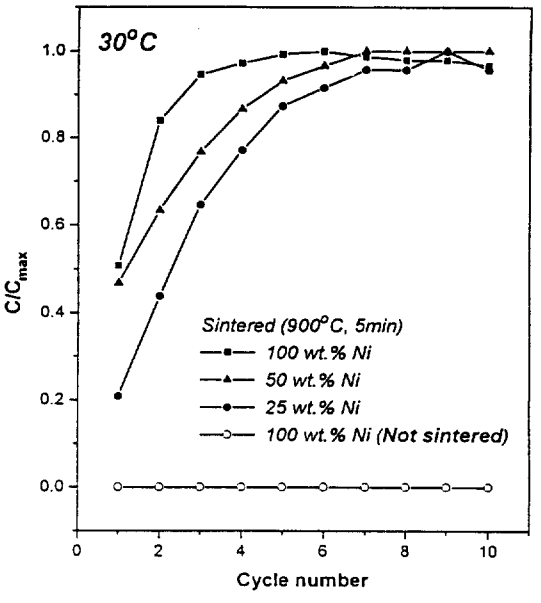

Fig. 1. Activation behaviors of $V_{0.9}Ti_{0.1}$-x wt.% Ni(x=25, 50, 100) alloys.

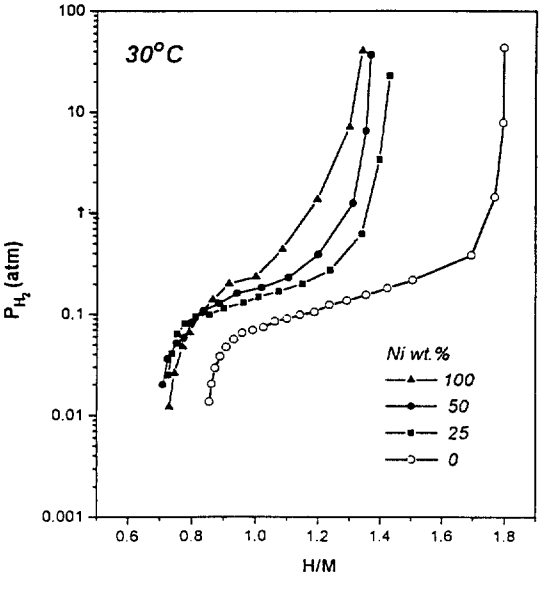

Fig. 2. Desorption PCT curves for $V_{0.9}Ti_{0.1}$-x wt.%Ni(x=0, 25, 20, 100) alloys sintered at 900℃ for 5 min.

3-2 Discharging efficiency

The pressure-composition desorption isotherms measured at 30℃ for the sintered $V_{0.9}Ti_{0.1}$-x wt.%Ni(x=0, 25, 50, 100) are shown in Fig. 2. In the $V_{0.9}Ti_{0.1}$ alloy which contains

no Ni, the hydrogen absorption capacity (H/M_{alloy}) and the effective hydrogen content(△[H/M]) are about 1.8 and 0.9, respectively. However, a clear decrease in the maximum hydrogen absorption capacity and effective hydrogen content have been observed in the $V_{0.9}Ti_{0.1}$-x wt.%Ni (x=25, 50, 100) alloy with increasing Ni content. The theoretical discharge capacity[4] per unit weight of the alloy was calculated as follows.

$$C_{th} = \frac{\triangle[H/M_{alloy}] \times F}{3.6 \times M_{alloy}} \quad (1)$$

; where C_{th}, F and M_{alloy} are the theoretical discharge capacity, the Faraday constant and the molecular weight of the alloy, respectively.

The theoretical discharges capacites of the alloys are shown in Table 1. The discharge characteristics of $V_{0.9}Ti_{0.1}$-x wt.%Ni(x=12.5, 25, 50, 100) after activa tion cycles are shown in Fig. 3, Fig. 4 and Fig. 8.

Table 1. Theoretical discharge capacities and effective hydrogen contents of $V_{0.9}Ti_{0.1}$-x wt.%Ni(x=0, 25, 50, 100) alloys sintered at 900℃ for 5 min.

Ni wt.%	0	25	50	100
Effective hydrogen content △[H/M]	0.92	0.66	0.6	0.45
Theoretical discharge capacity(mAh/g)	490	350	315	240

In Fig. 3, the absolute value of the discharge potential was increased with increasing Ni content, and the discharge capacities of the electrodes showed a maximum value with respect to the Ni content, as shown in Fig. 4. The optimal amount of Ni powder showing the highest discharge capacity of 302 mAh/g has been found to be 25 wt.%

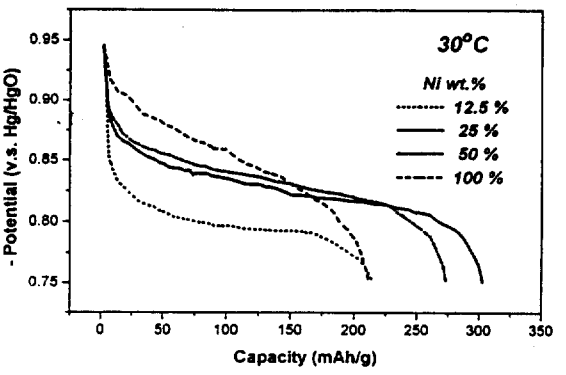

Fig. 3. Discharge curves for $V_{0.9}Ti_{0.1}$-x wt.%Ni(x=12.5, 25, 50, 100) after activation cycling.

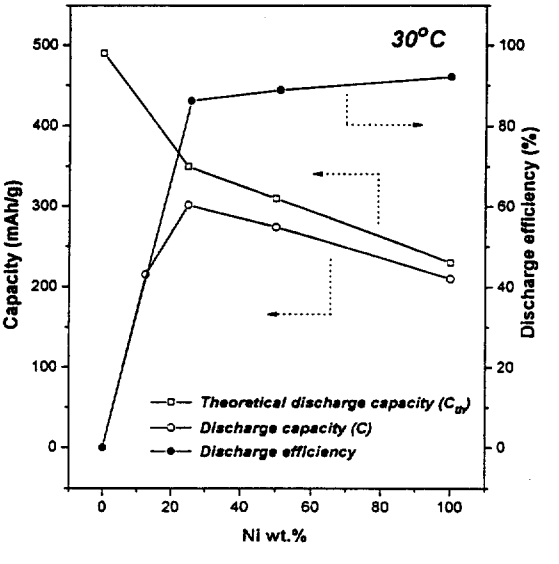

Fig. 4. Theoretical discharge capacity, discharge capacity and discharge efficiency of $V_{0.9}Ti_{0.1}$ alloy with Ni content.

The discharge efficiencies of the $V_{0.9}Ti_{0.1}$ alloy electrodes are also shown in Fig. 4. The

discharge efficiency can be writtern in the following form.

$$\text{Discharge efficiency} = \frac{C}{C_{th}} \times 100(\%) \qquad (2)$$

; where C is the discharge capacity measured at discharge current of 50 mA/g($V_{0.9}Ti_{0.1}$ alloy) and C_{th} are the theoretical discharge capacity calculated from equation(1). The discharge efficiency of $V_{0.9}Ti_{0.1}$ electrodes was improved with increasing Ni.

3-3 X-ray and SEM(EDS) analysis

The X-ray diffraction patterns of $V_{0.9}Ti_{0.1}$ alloy sintered with 100 wt.% Ni powder are shown in Fig. 5. The $V_{0.9}Ti_{0.1}$ alloy and Ni powder peaks represent the typical BCC and FCC structures respectively, and there appears four new peaks represenenting VNi_3 phase. As the sintering time increases, the amount of VNi_3 phase increased. As this phase cannot absorb hydrogen because of too high nickel content, the formation of VNi_3 phase will decrease the theoretical discharge capacities of the electrodes.

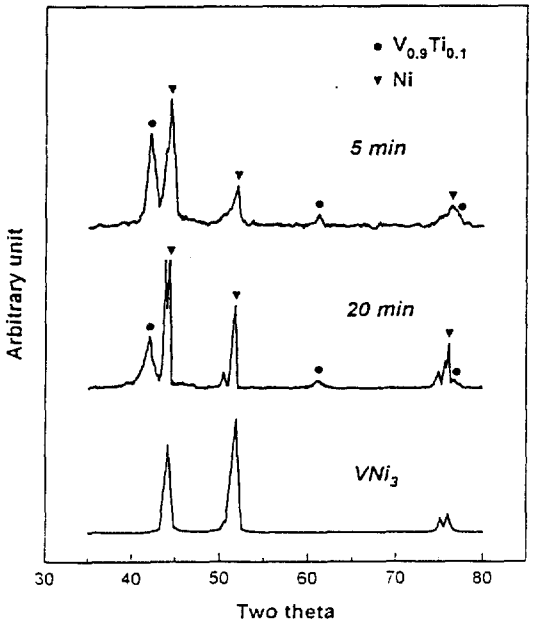

Fig. 5. X-ray diffraction patterns of $V_{0.9}Ti_{0.1}$-100 wt.%Ni alloy sintered at 900℃ and VNi_3.

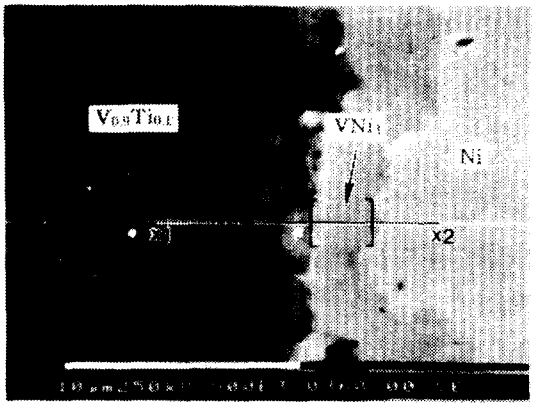

(A)

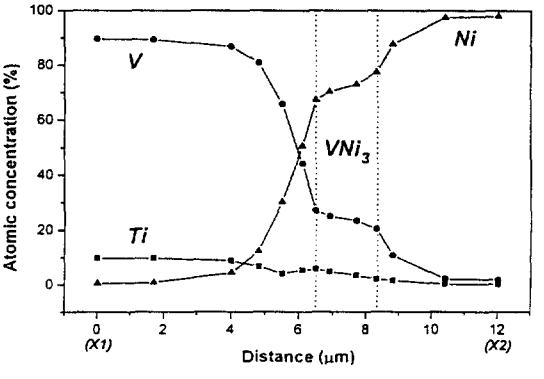

(B)

Fig. 6. (A) SEM image of $V_{0.9}Ti_{0.1}$-25 wt.%Ni alloy sintered at 900℃ for 5 min.
(B) EDS analysis of $V_{0.9}Ti_{0.1}$-25 wt.%Ni alloy sintered at 900℃ for 5 min. $V_{0.9}Ti_{0.1}$-x wt.%Ni(x=0, 25, 50, 100)

The surface morpholorgy of the $V_{0.9}Ti_{0.1}$

alloy sintered at 900℃ for 5 min with 25wt.% Ni powder is shown in Fig. 6(A). The second phase is observed between $V_{0.9}Ti_{0.1}$ and Ni phase with the thickness of 2-3 μm. The second phase has been proved to be VNi_3 from EDS analysis as shown in Fig. 6(B). In the second phase the ratio of Ni to V is appro- ximately three. At the same sintering condition (at 900℃ for 5 min), as the amount of Ni powder increases, the electrochemical effici-encies are improved by VNi_3 and Ni phase whilst the hydrogen storage capacity decreases. As a result, the discharge capacity showes maximun value with respect to Ni content. it is well known that the VNi_3 hardly absorbed hydrogen, so the theoretical discharge capacity of the electrode is de-creased by the formation of VNi_3. However, as it has an excellent catalytic activity[9] on the absorption/desorption of hydrogen in KOH electrolyte, the electrochemical efficiencies are improved by VNi_3 and Ni phase.

3-4. Exchange current density

The catalytic activity of the VNi_3 phase has been clarified in by measuring exchange current density of the electrodes. In general, the exchange current density is calculated on the basis of surface area of electrodes. how-ever, It is hard to measure the surface area of electrodes because the surface areas of electrodes increased during activation cycling by continuous micro creaking. So, in this experiment, the values of the exchange current densities are normalized by the weight of $V_{0.9}Ti_{0.1}$ alloy, i.e. current/g of $V_{0.9}Ti_{0.1}$ alloy. The exchange current densities of $V_{0.9}Ti_{0.1}$ -x wt.%Ni(x=0, 12.5, 25, 50, 100) are shown in Fig. 7. The exchange current density increased with the increase of Ni content.

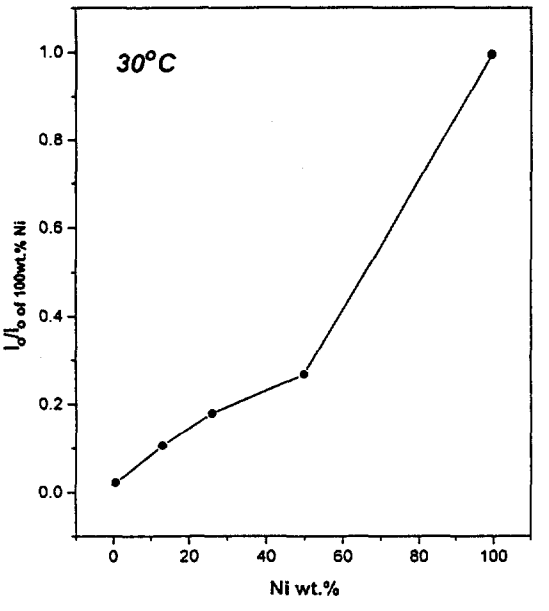

Fig. 7. Exchange current densities of $V_{0.9}Ti_{0.1}$-x wt.%Ni(x=0, 12.5, 25, 50, 100) alloys sintered at 900℃ for 5 min.

3-5. Discharge overpotential

In order to identify the electrochemical characterstics of VNi_3 phase, the discharge overpotential of the electrodes has been measured. The discharge overpotential can be written in the following form:

$$\text{Discharge overpotential} = | V_{real} - V_{eq} | \quad (3)$$

$$V_{eq} = -0.9409 - 0.0301 \times \log P_{H_2} \text{(v.s. Hg/HgO, at 30℃, PH=14)} \quad (4)$$

The values of V_{eq}[10] are obtained by the potential calculated from the pressure at the

middle of plateau region in each PCT curves by Nernst(eq. 4). The value of V_{real} are directly obtained by the potential at the middle of each discharge curves. The discharge overpotentials of $V_{0.9}Ti_{0.1}$-x wt.%Ni(x =25, 50, 100) are shown in Fig. 8. As the amount of Ni powder increases, the discharge overpotential decreases. However, it is not clear whether this decrease of discharge overpotential was due to the VNi_3 phase or due to the sintered Ni phase. In order to clarify which phase is more dominant, the amount of VNi_3 phase has been changed

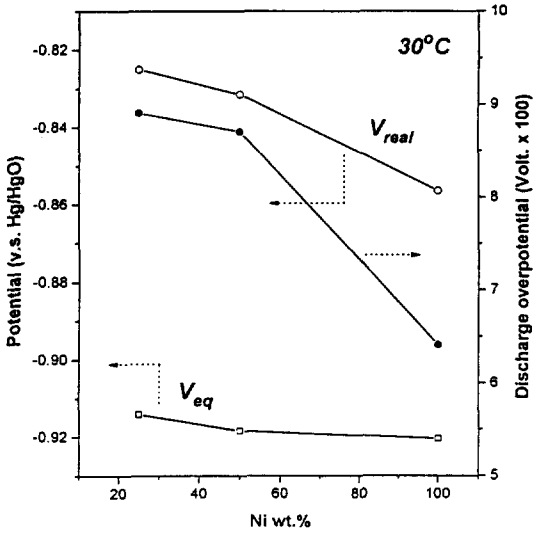

Fig. 8. Discharge overpotentials of $V_{0.9}Ti_{0.1}$-x wt.%Ni(x=25, 50, 100) alloys sintered at 900℃ for 5 min.

keeping the total weight of Ni powder constant. The PCT curves and discharge curves of the $V_{0.9}Ti_{0.1}$ alloy sintered with 100wt.%Ni powder at 900℃ for 5min and 25min are shown in Fig. 9 and Fig. 10,

respectively. The values of V_{eq} are obtained

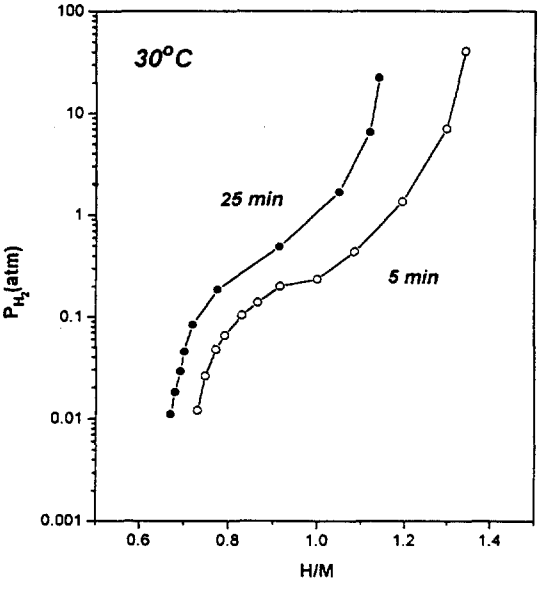

Fig. 9. Desorption PCT curves of the $V_{0.9}Ti_{0.1}$-100 wt.%Ni alloys sintered at 900℃ for 5 min and 25 min.

from these PCT curves. The discharge overpotential of $V_{0.9}Ti_{0.1}$-100wt.% alloy sintered for 5 and 25 min. are shown in Fig. 11. As

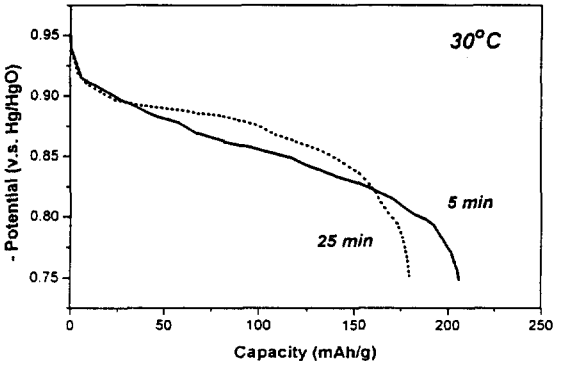

Fig. 10. Discharge curves of $V_{0.9}Ti_{0.1}$-100 wt.% Ni alloys sintered at 900℃ for 5 min and 25 min.

the sintering time increased, the discharge overpotential decreased. So, the decrease of the discharge overpotential is thought to be attributed to the increased amount of the VNi_3 phase.

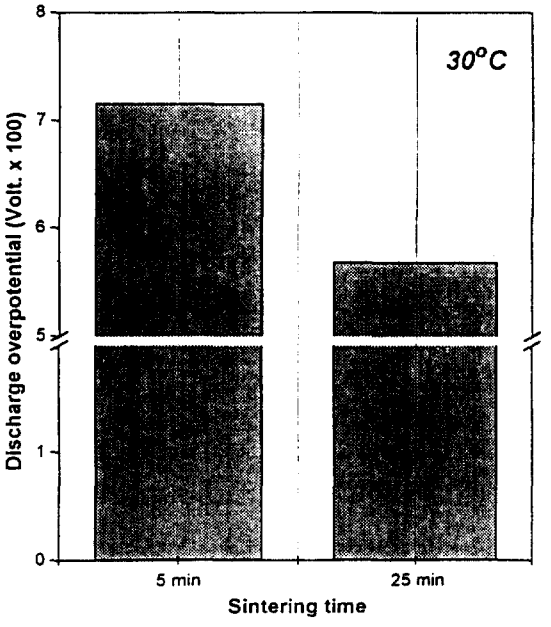

Fig. 11. Discharge overpotentials of $V_{0.9}Ti_{0.1}$-100 wt.%Ni alloys sintered at 900℃ for 5 min and 25 min.

4. Conclusions

By surface modification, the anode material for Ni-MH battery has developed using $V_{0.9}Ti_{0.1}$ alloy which has not been used for anode material due to the poor discharge characteristics. In this new surface modification process, $V_{0.9}Ti_{0.1}$ alloy powder has been sintered with Ni powder at 900℃ for 5 min changing the weight of Ni powder. The electrodes have been activated within 10 cycles in KOH electrode. As the amount of nickel powder increased, the electrochemical efficiencies were improved whilst the hydrogen storage capacity decreased. As a result the discharge capacity showed maximum value of 302 mAh/g at 25wt% Ni content. From X-ray and SEM(EDS) analysis, the second phase was observed and it has been found to be VNi_3. As VNi_3 hardly absorbs hydrogen, the theoretical capacity of the electrode is decreased by the formation of VNi_3 phase. The electrochemical effects of VNi_3 is found to be more dominant than those of sintered Ni phase

References

1. H. F. Bittner and C. C. Badcock, J. Electrochemical. Soc., Vol. 130, 193C (1983)
2. J. J. G. Willems and K. H. J. Bushow, J. Less-Common met., 129, 13(1987)
3. M. A. Fetcenko, S. Venkatesan and S. R. Ovshinsky, Proc. Int. Symp. on Metal-Hydrogen System, Upssala, June 1992, PII. 96.
4. J. J. G. Willems, Philips J. Res., 39, Suppl. No. 1 (1984)
5. S. Wakao, H. Sawa and J. Furukawa, J. Less-Common Met., 172-174, 1219 (1991)
6. T. Sakai, H. Yoshinaga, H. Miyamura, N. Kuriyama and H. Ishikawa, J. Alloys and Compounds, 180, 37-54 (1992)
7. S. R. Kim and J. Y. Lee, J. Alloys and Compounds, 210, 109-113 (1994)

8. J. F. Lynch, A. J. Maeland and G. G. Libowitz, Z. Phys. Chem. N. F., 145, 51 (1985)
9. M. M. Jaksic, Int. J. Hydrogen Energy, Vol 12, No. 11, 727 (1987)
10. S. R. Kim, Ph. D. Thesis, KAIST, Taejon, korea(1993)